The localization of phonons in ion traps with controlled quantum disorder



2010 New J. Phys. 12 123016

(http://iopscience.iop.org/1367-2630/12/12/123016)

New Journal of Physics
The open-access journal for physics

# The localization of phonons in ion traps with controlled quantum disorder

**A Bermudez**[1], **M A Martin-Delgado and D Porras**
Departamento de Física Teórica I, Universidad Complutense, 28040 Madrid, Spain
E-mail: bermudez.carballo@gmail.com

*New Journal of Physics* **12** (2010) 123016 (10pp)
Received 10 September 2010
Published 9 December 2010
Online at http://www.njp.org/
doi:10.1088/1367-2630/12/12/123016

**Abstract.** We show that the vibrations of a chain of trapped ions offer an interesting route to explore the physics of disordered quantum systems. By preparing the internal state of the ions in a quantum superposition, we show how the local vibrational energy becomes a stochastic variable, its statistical properties inherited from the underlying quantum parallelism of the internal state. We describe a minimally perturbing measurement of the resonance fluorescence, which allows us to study effects such as Anderson localization without the need for ground-state cooling or individual addressing and thus paves the way for high-temperature ion experiments.

**Contents**



[1] Author to whom any correspondence should be addressed.

Disorder in quantum systems leads to a variety of fascinating phenomena. In particular, the disorder-induced localization of particles has been the focus of intense theoretical and experimental research since its discovery by P W Anderson [1]. Experiments have been performed in a variety of setups involving electronic transport [2], propagation of light [3] or sound waves [4] and disordered Bose–Einstein condensates [5, 6]. So far, any experiment has limitations in the degree of control of particle interactions or the statistical properties of disorder. Realizations of the most challenging situations therefore remain elusive, for example Anderson localization in the presence of correlated disorder or controlled interactions. In this paper, we show that the vibrations of an ion crystal can be used to study the physics of Anderson localization. The ability to control the interactions and measure the state of trapped ions [7] makes this setup an ideal quantum simulator of many-body systems (see e.g. [8]–[11]), as recently shown in experiments [12, 13]. Our proposal relies on a description of the radial vibrations of an ion chain in terms of weakly coupled harmonic oscillators [9]. These vibrations are coupled by means of lasers to the internal states of the ions, represented by a set of two-level systems, or effective spins. We employ a state-dependent Stark-shift that shifts the local ion trapping potential to couple spins and phonons. This composite system can be described effectively as two different species interacting in a chain. Since the spin species is the slowest, it behaves like a frozen background for phonons and makes the local phonon energy a true stochastic variable whose statistical properties are determined by the spin quantum state.

In particular, we show the following. (i) By preparing the ion internal state in a quantum superposition corresponding to a separable state, disorder leads to the localization of phonons. This effect can be directly measured by studying the propagation of phonons along the chain. (ii) Fundamental properties, such as the phonon localization length, may be detected even at high temperatures, and without the need to resolve individual ions. This is achieved by measuring the resonance fluorescence. (iii) Our proposal can be extended to implement a variety of interesting situations, such as binary-correlated disorder, or localization in the presence of anharmonicities.

## 1. The general scheme

We consider a chain of $N$ ions with mass $m$ and charge $e$ trapped by harmonic potentials. The ions are coupled by the Coulomb interaction, and thus their displacements around the equilibrium positions are described by collective vibrational modes. In particular, we focus on the vibrations in the radial—transverse to the chain—direction. Each ion also has two internal levels ($|0\rangle$, $|1\rangle$) with energy difference $\omega_0$. Thus, the system Hamiltonian is (we set $\hbar = 1$)

$$H_0 = \omega_0 \sum_{j=1}^{N} \sigma_j^z + \sum_{n=1}^{N} \Omega_n a_n^\dagger a_n, \qquad \Omega_n^2 = \omega_t^2 \left(1 + \beta \mathcal{V}_n\right), \tag{1}$$

where $\sigma_j^z = |0_j\rangle\langle 0_j| - |1_j\rangle\langle 1_j|$, $a_n^\dagger$ ($a_n$) create (annihilate) radial phonons in the vibrational mode $n$, and $\Omega_n$ are the radial-mode energies determined by the trapping frequency $\omega_t$ and the harmonic correction $\mathcal{V}_n$. The latter is obtained from the diagonalization of $V_{jk} = |j-k|^{-3}(1-\delta_{jk}) - \sum_{l\neq j} |j-l|^{-3}\delta_{jk}$, such that $\mathcal{V}_n = \sum_{jk} \mathcal{M}_{jn} V_{jk} \mathcal{M}_{kn}$, where $\mathcal{M}_{jn}$ are the phonon wavefunctions. Finally, the ratio of the Coulomb repulsion to the trapping energy $\beta = e^2/m\omega_t^2 a^3$ fulfills $\beta \ll 1$, such that the ions correspond to weakly coupled oscillators [9]. We work under the simplification of equally spaced ions, although our results can be easily extended to inhomogeneous chains.

**Table 1.** Spin, phonon and spin–phonon coupling strengths.

| | | |
|---|---|---|
| $\omega_j = \omega_t - \sum_{l\neq j} \frac{t}{\lvert j-l\rvert^3}$ | $\omega_j \sim \omega_t$ | $\omega_t \sim 10^4$ kHz |
| $t_{jk} = \frac{t}{\lvert j-k\rvert^3}$ | $t = \beta\omega_t$ | $t \sim 10^2$ kHz |
| $U_j = U$ | $U = -\frac{F^2}{\delta}$ | $U \sim 10$ kHz |
| $J_{jk} = \frac{J}{\lvert j-k\rvert^3}$ | $J = \frac{F^2}{\delta^2}\beta\omega_t$ | $J \sim 1$ kHz |

We use a laser in the radial direction with frequency $\omega_L$ and wavevector $k_L$, which is nearly resonant to a narrow transition between the internal states. Thus, the vibrational sidebands can be resolved, and the laser couples spins and phonons through the spatial dependence of the dipole coupling $H_L = \frac{\Omega_L}{2}\sigma_j^+ e^{ik_L x_j - i\omega_L t} + \text{h.c.}$, where $\sigma_j^+ = |1_j\rangle\langle 0_j|$. In the limit $\beta \ll 1$, $\omega_L$ can be tuned near resonance with all the modes by choosing $\omega_L - \omega_0 = -\Omega_n + \delta_n$, and detunings $\delta_n \ll \Omega_n$. Expressing the radial coordinate as $x_j = \sum_n \mathcal{M}_{jn}(a_n + a_n^\dagger)/\sqrt{2m\Omega_n}$, the coupling can be approximated by a multimode red-sideband Hamiltonian. Here, one considers $\Omega_L \ll \Omega_n$ and $\eta_n = k_L/\sqrt{2m\Omega_n} \ll 1$, where the carrier and remaining sidebands can be neglected, and the Hamiltonian in the interaction picture with respect to $H_0$ reads

$$H_{\text{int}}(t) = \sum_{jn} F_{jn}\sigma_j^+ a_n e^{-i\delta_n t} + \text{H.c.}, \qquad F_{jn} = \frac{i\Omega_L}{2}\eta_n \mathcal{M}_{jn}. \tag{2}$$

Under the condition $|F_{jn}| \ll \delta_n$, we obtain an effective Hamiltonian from the corrections to second order in $|F_{jn}|/\delta_n$,

$$H_{\text{eff}} = H_0 + \sum_{jkn} \lambda_{jkn}\sigma_j^+\sigma_k^- + \sum_{jnm} \kappa_{jnm}\sigma_j^z a_n^\dagger a_m, \tag{3}$$

where $\lambda_{jkn} = 2F_{jn}F_{kn}^*/\delta_n$ is an effective coupling mediated by the vibrational modes, and $\kappa_{jnm} = -F_{jn}F_{jm}^*(\delta_n + \delta_m)/2\delta_n\delta_m$ stands for the spin–phonon coupling. Equation (3) can be recast in terms of local modes, $a_j = \frac{1}{2}\sum_n \mathcal{M}_{jn}(\Delta_n^+ a_n + \Delta_n^- a_n^\dagger)$, with $\Delta_n^\pm = (\frac{\omega_t}{\Omega_n})^{1/2} \pm (\frac{\Omega_n}{\omega_t})^{1/2}$. In the limit $\beta \ll 1$, the Hamiltonian can be split into three different terms: $H_{\text{eff}} = H_p + H_s + H_{s-p}$,

$$\begin{aligned} H_p &= \textstyle\sum_j \omega_j a_j^\dagger a_j + \sum_{jk} t_{jk} a_j^\dagger a_k, \\ H_s &= \textstyle\sum_j \omega_0 \sigma_j^z + \sum_{jk} J_{jk}\sigma_j^+\sigma_k^-, \qquad H_{s-p} = U\sum_j \sigma_j^z a_j^\dagger a_j. \end{aligned} \tag{4}$$

The last expression has a clear physical meaning: $H_p$ is an effective tight-binding Hamiltonian describing the harmonic coupling between ions in terms of phonon hopping; $H_s$ stands for a dipolar $XY$-model of spins subjected to a longitudinal field; and $H_{s-p}$ is spin–phonon coupling induced by a state-dependent Stark-shift of the local ion energy [14]. For non-resolved sidebands, this term would correspond to a spin-dependent light force that does not involve the phonon modes [15]. Typical values for the coupling constants in equation (4) depend on $F = \Omega_L\eta_L/2$, $\eta_L = k_L/\sqrt{2m\omega_t}$ and $\delta = \omega_L - \omega_0 + \omega_t$ (see table 1).

The Hamiltonian in equation (4) corresponds to a chain with two species (phonons and spins), coupled by a density–density interaction. By choosing $\omega_t \sim 10$ MHz, $\delta \sim 1$ MHz, $\beta \sim 0.05$ and $F \sim 0.1\delta$, we obtain the hierarchy of coupling strengths $t \sim 100\,\text{kHz} \gg U \sim 10\,\text{kHz} \gg J \sim 1$ kHz. Accordingly, the spin dynamics are much slower than the typical phonon time scales, such that spins may serve as an auxiliary system to induce a disordered background for phonons. Note that the separation in time scales is a consequence of the fact that we consider

the limit $(F/\delta)^2 \ll 1$. In this limit, induced effective spin–spin interactions are suppressed with respect to the phonon couplings, $J = (F/\delta)^2 t$. A similar situation has also been studied for atom mixtures in optical lattices [16], whereas the effect of randomness on quantum networks was addressed in [17].

## 2. Controlled disorder

We consider the initial state $\rho(0) = \rho_s^0 \otimes \rho_p^0$, where $\rho_s^0 = |\Psi_s\rangle\langle\Psi_s|$ is an arbitrary pure state with $|\Psi_s\rangle = \sum_{\{s\}} c_{\{s\}} |\{s\}\rangle$. The set $\{s\} = \{s_1, \ldots, s_N\}$, with $s_j \in \{0, 1\}$, defines a given spin configuration, and $c_{\{s\}} \in \mathbb{C}$ are the corresponding probability amplitudes. Due to the quenching of the spin dynamics, the phonon evolution can be approximated by $\rho_p(t) = \sum_{\{s\}} |c_{\{s\}}|^2 \, \mathrm{e}^{-\mathrm{i}H_{\mathrm{eff}}^{\{s\}} t} \rho_p^0 \, \mathrm{e}^{\mathrm{i}H_{\mathrm{eff}}^{\{s\}} t}$, where

$$H_{\mathrm{eff}}^{\{s\}} = H_p + H_{s-p}^{\{s\}} = \sum_{jk} t_{jk} a_j^\dagger a_k + \sum_j \varepsilon_j(\{s\}) a_j^\dagger a_j, \tag{5}$$

and $\epsilon_j(\{s\}) = \omega_j + U(1 + 2s_j)$ is an on-site energy with two possible values $\varepsilon_j = \omega_j \pm U$. Due to the underlying quantum parallelism, the system explores simultaneously all realizations of the on-site energy with probabilities $p(\varepsilon_j(\{s\})) = |c_{\{s\}}|^2$. We stress that the binary randomness inherited from the frozen-spin background can be engineered at will by preparing different internal states $|\Psi_s\rangle$. In principle, arbitrary quantum states can be prepared by trapped-ion quantum logic [19]. Therefore, we obtain a versatile phonon model with diagonal disorder, formally equivalent to the so-called random binary alloy (RBA) [18], but in stark contrast, we can externally control the disorder (see figure 1(a)). Note that the long-range hopping in equation (4) does not change qualitatively the phase diagram of the model.

## 3. Anderson localization in the random binary alloy (RBA) model

In the absence of disorder, phonon wavefunctions are extended over the whole ion chain. Conversely, impurities lead to interference phenomena of back-scattered waves that might localize the phonon wavefunctions. This effect, known as Anderson localization, occurs for any amount of disorder in one-dimensional (1D) systems [20]. In contrast to impurities that may consist of ions with a different mass [15], we consider here the spin ensemble as a source of disorder. As an illustrative example, we focus on the RBA model with uncorrelated disorder, and choose a separable initial spin state $\rho_s^0 = \otimes_j |+_j\rangle\langle+_j|$, with $|+_j\rangle = \left(|0_j\rangle + |1_j\rangle\right)/\sqrt{2}$. The latter can be prepared by means of a laser or microwave field addressed to the internal transition of each ion [7]. Note that such a state leads to a flat probability distribution of the local phonon energies in equation (5), which is characterized by $p(\varepsilon_j(\{s\})) = 1/2^N$. In order to observe localization of phonons, we can study either the dynamics of single phonon excitations or the spectral properties of a thermal distribution of phonons. Below, we describe these two possible routes.

### *3.1. Direct measurement of localization*

The experimental techniques required for creating and measuring the quantum state of motion have been demonstrated with single ions [21]. In this case, we also need cooling close to

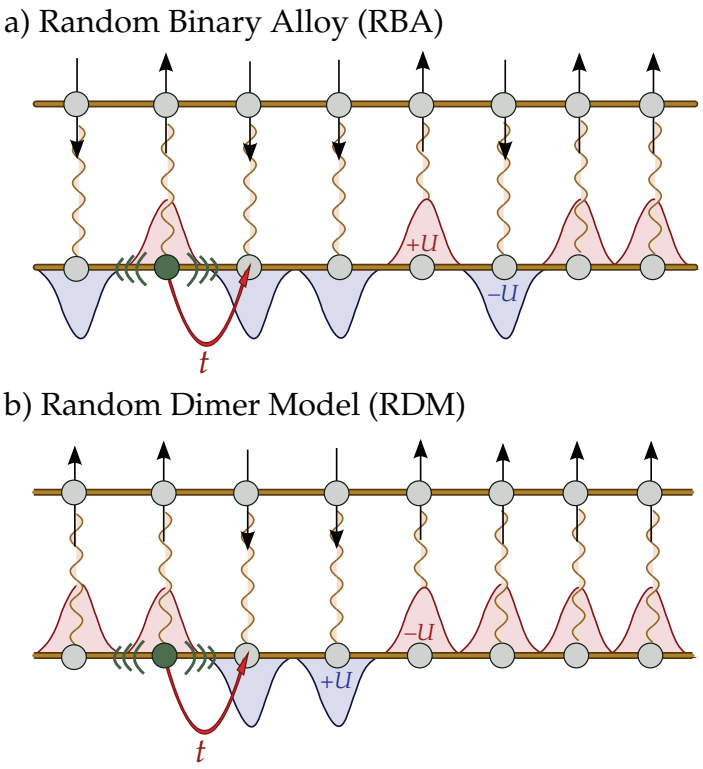


**Figure 1.** Disordered ion chain as a virtual two-leg ladder composed of a frozen-spin ensemble locally coupled to a system of hopping phonons. (a) Uncorrelated RBA. (b) Correlated random dimer model (RDM).

the vibrational ground state and individual addressing of ions. To create a single phonon in an ion on the chain, we assume an experimental procedure that is faster than the time scale for phonon tunneling, $1/t$. This is in principle feasible, since sidebands can be resolved on time scales longer than $1/\omega_{\rm t}$. Considering a time scale $t_{\rm p}$ for the pulse sequence required for creating a single phonon, and typical values $\omega_{\rm t} = 10\,{\rm MHz}$ and $t = 100\,{\rm kHz}$, the required condition $1/\omega_{\rm t} \ll t_{\rm p} \ll 1/t$ may be fulfilled. Note that this is in agreement with the time scales shown in [21]. The experiment should proceed as follows. (i) Laser cooling close to the ground state, where the required mean phonon number $\bar{n} \ll 1$ may be achieved by sideband cooling without individual resolution of the vibrational modes. (ii) Initialization, where a single phonon localized at a given site $l$ is created by a red-sideband coupling (single-ion version of equation (2)) that drives the transition $|1_l\rangle \otimes |{\rm vac}\rangle_{\rm p} \to |0_l\rangle \otimes a_l^\dagger |{\rm vac}\rangle_{\rm p}$, where $|{\rm vac}\rangle_{\rm p}$ is the phonon vacuum. Afterwards, internal states should be prepared in the coherent superposition $|+_j\rangle$. (iii) Switch on the disorder on-site phonon energies in equation (5), and wait for single-phonon propagation along the chain until a given final time $t_{\rm f}$. (iv) Infer the phonon number by measuring the excitation probability of internal states. In the absence of disorder, the long-time dynamics at $t_{\rm f} \gg \max\{1/\Omega_n\}$ correspond to a quantum random walk where the phonon diffuses over the entire chain. Conversely, disorder yields a drastically different behavior as shown in the numerical results of figure 2, where phonons are confined within a localization length $\xi_{\rm l} \approx 10$ sites.

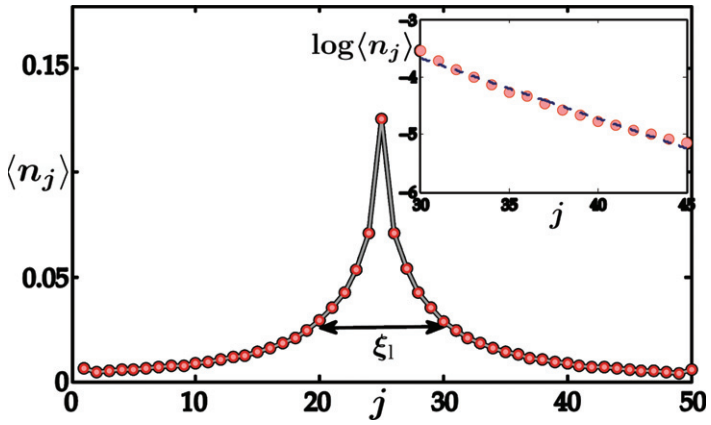


**Figure 2.** Mean phonon number $\langle n_j(t_f)\rangle$ at $t_f = 10^3/\beta\omega_t$, for a disordered chain, $U = 3t/4$, with $N = 50$ ions. A localized phonon at the center of the chain does not spread completely, but remains localized within the length scale $\xi_l$. Inset: exponential tail of the distribution that gives us the localization length, $\xi_l = A^{-1} \approx 10 \ll N$.

### *3.2. Spectral measurement of localization*

In the following, we show how to measure phonon spectral properties. Our scheme perturbs the spins minimally, such that we remain in the quenched disorder limit implicit in equation (5). For this purpose, we propose to measure the fluorescence from a cycling transition, and show how to get the phonon localization length out of it, without either cooling to the ground state or individual addressing. To describe the measurement scheme, we extend the theory of resonance fluorescence from a single atom [23] to an ion chain. A laser with wavevector $\mathbf{k}_c$ in the radial direction drives a cycling transition between levels $|1_j\rangle$ and $|a_j\rangle$, with detuning $\Delta$ and Rabi frequency $\Omega_c$. Photons with momentum $-\mathbf{k}_c$ are detected (see figure 3(a)). We consider the limit $\Gamma \gg \Delta \gg \Omega_c/2$, where $\Gamma$ is the natural linewidth of the cycling transition. In this limit, the excited level $|a_j\rangle$ can be adiabatically eliminated and we obtain the following coupling between the ions and the fluorescence photons:

$$\begin{aligned} H_{\rm cyc}(t) &= \sum_{j,\mathbf{q}\approx\mathbf{k}_c} g_{\mathbf{q}} O_j c_{\mathbf{q}}^\dagger \, e^{i(\omega_{\mathbf{q}}-\omega_L)t} + \text{H.c.}, \\ O_j &= i\frac{\Omega_c}{\Gamma} e^{i2k_L x_j} |1_j\rangle\langle 1_j| \\ &= i\frac{\Omega_c}{\Gamma}(1 + 2i\eta_c(a_j + a_j^\dagger))|1_j\rangle\langle 1_j| + O(\eta_c^2), \end{aligned} \tag{6}$$

where $c_{\mathbf{q}}^\dagger$ ($c_{\mathbf{q}}$) create (annihilate) photons with momentum $\mathbf{q}$, $g_{\mathbf{q}}$ is the dipole coupling of the cycling transition and $\eta_c = k_c/\sqrt{2m\omega_t}$. Equation (6) describes photon emission weighted by $\Omega_c/\Gamma$, the probability amplitude for occupation of $|a_j\rangle$. The fluorescence spectrum is given by $\mathcal{S}(\omega) = \lim_{T\to\infty} \frac{1}{2\pi T} \int_0^T dt \int_0^T d\tau \sum_{jl} \langle O_j^\dagger(t) O_l(t+\tau)\rangle e^{i(\omega-\omega_L)\tau}$, (see for example [24]). Near $\omega = \omega_L \pm \omega_t$ the fluorescence is given by the sum of contributions from different vibrational modes.

To be specific, we compute the resonance fluorescence spectrum from a phonon distribution at fine temperature $T$ after the Doppler cooling. In this limit, collective vibrational modes are not

resolved, and thus the phonon density matrix describes a set of individual harmonic oscillators, $\rho_{\rm p} = \mathcal{Z}^{-1}\exp(-\frac{\omega_t}{T}\sum_j a_j^\dagger a_j)$. The fluorescence spectrum is then

$$\mathcal{S}_\pm(\omega) = \mathcal{S}_0^\pm \sum_{\{s\}} |c_{\{s\}}|^2 \sum_{jln} s_j s_l \mathcal{M}_{jn}^{\{s\}} \mathcal{M}_{ln}^{\{s\}} \delta(\omega - \omega_{\rm L} \pm \Omega_n^{\{s\}}), \tag{7}$$

where $\mathcal{S}_0^+ = \mathcal{S}_0\bar{n}$, $\mathcal{S}_0^- := \mathcal{S}_0(\bar{n}+1)$. Until now, we have neglected the broadening of the spectral delta functions by the heating rates. This effect is discussed below.

Let us show how equation (7) allows us to determine the phonon localization length. We focus on the center-of-mass (COM) mode ($n = 0$), which has the highest energy. In the absence of disorder, the fluorescence COM peak intensity fulfills $\sum_{\{s\}} |c_{\{s\}}|^2 \sum_{jl} s_j s_l \mathcal{M}_{j0}\mathcal{M}_{l0} = \frac{1}{4}(N+1)$, because $\mathcal{M}_{j0} = 1/\sqrt{N}$. Therefore, the peak at the COM frequency scales linearly with the number of ions, $\mathcal{S}_-(\omega) \propto N\delta(\omega - \omega_{\rm L} - \Omega_{\rm com})$. Conversely, for any amount of disorder, wavefunctions become exponentially localized [20]. Since the wavefunction of phonons close to the COM frequency now has a spatial extent of the order of the localization length $\xi_l$, we expect the COM fluorescence peak to saturate to $\mathcal{S}_-(\omega) \propto \xi_l\delta(\omega - \omega_{\rm L} - \Omega_{\rm com})$ when $N \gg \xi_l$. Thus, by studying the scaling of the COM peak with the number of ions in the chain, the saturation of the intensity will reveal the Anderson localization length. We illustrate our method with a numerical calculation in figures 3(b) and (c), where the blue sideband fluorescence is represented with and without disorder. Localization is evident already with a moderate ion number $N \approx 20$.

We now discuss a few points on the measurement of resonance fluorescence. Note that the sideband contributions to the resonance fluorescence spectrum have a linewidth of the order of the cooling/heating rates, $\Gamma_{\rm h/c}$, as shown, for example, in [23]. The sideband spectrum can be obtained with a heterodyne detection scheme, as discussed in [22]. During the measurement, radial motion of the ion chain may be heated or cooled with a rate of the order of $\Gamma_{\rm h/c} = \eta_{\rm L}^2\Omega_{\rm c}^2/\Gamma$. In a typical cycling transition, we find that $\Gamma \gg \omega_x$. By choosing $\Delta = \omega_x$, the experiment is in the Doppler cooling regime, such that in the steady state the mean phonon number has typical values $\bar{n} = 10$ [7]. Thus, the resonance fluorescence can be measured with a steady phonon number within the Lamb–Dicke regime. In addition to that, Doppler cooling leads to the broadening of vibrational sidebands in equation (7). However, this effect does not spoil the measurement as long as $\Gamma_{\rm h/c}$ is of the order of the separation between vibrational modes, in which case broadening will not significantly affect the scaling of photoluminescence. Finally, note that decoherence of the internal states is allowed in our proposed experiment, since quantum coherence is not required for the effective spins to induce a disordered potential in equation (5).

## 4. Localization–delocalization transition

The localization paradigm is altered by the presence of strong interactions or correlated disorder, which lead to a variety of phases where a localization–delocalization transition holds. In the following, we show how to use our scheme to realize those situations.

### *4.1. Correlated disorder*

In addition to the uncorrelated disorder discussed above, entanglement in $|\Psi_{\rm s}\rangle$ leads to correlated disorder in the phonon Hamiltonian. The simplest situation consists of local vibrational energies, which take on two possible values, namely $\varepsilon_j = \omega_j \pm U$, with the

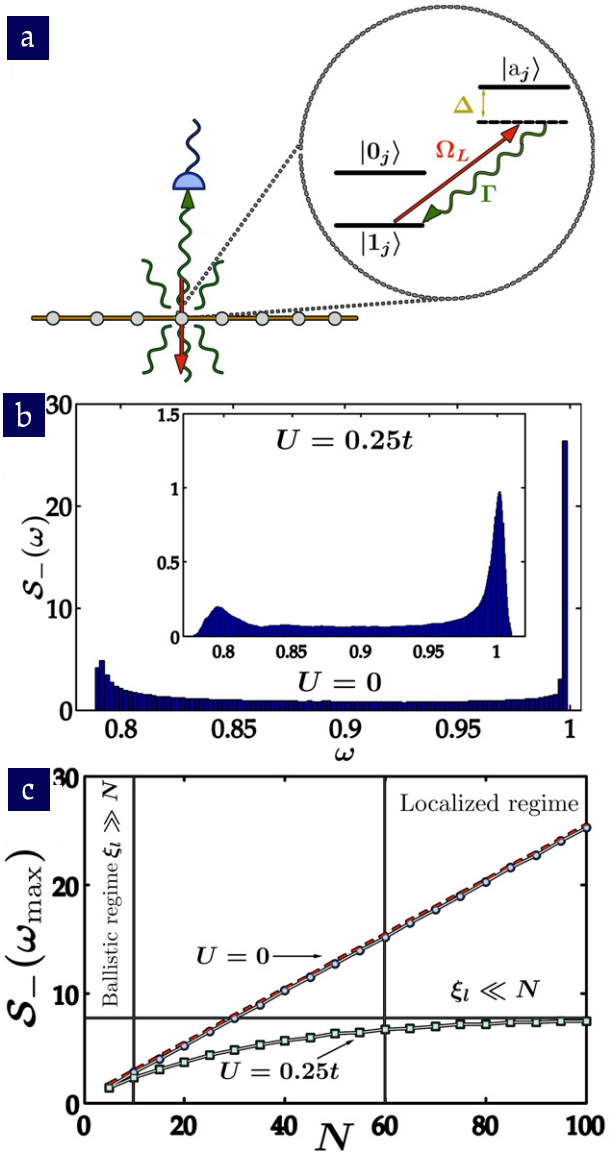


**Figure 3.** (a) Scheme of the cycling transition coupling the ion selectively $|1_j\rangle$ to $|a_j\rangle$. Selection rules impose the decay back to $|1_j\rangle$. (b) Fluorescence $\mathcal{S}_-(\omega)$ (units of $\mathcal{S}_0^-$) as a function of $\omega$ (units of $\omega_t$) for a chain of $N = 100$ and $\beta = 0.05$. The main figure: the ordered case $U = 0$. Inset: the disordered regime $U/t = 0.25$. (c) Scaling of the fluorescence for $\beta = 0.05$. Blue circles: the ordered regime $U = 0$, which agrees with $\mathcal{S}_-(\Omega_{\rm com}) \propto \frac{1}{4}(1 + N)$ (red dashed line). Green squares: disorder $U/t = 0.25$, where saturation shows phonon localization.

constraint $\varepsilon_j = \varepsilon_{j+1}$ for $j$ odd (see figure 1(b)). This is known as the RDM [25]. To induce such correlations, one should use quantum gates to prepare Bell pairs $|\Psi_s\rangle = \otimes_{j=\rm odd}|\Phi_j^+\rangle$, where $|\Phi_j^+\rangle = (|0_j\rangle|0_{j+1}\rangle + |1_j\rangle|1_{j+1}\rangle)/\sqrt{2}$. Interestingly, this model presents a quantum phase transition between an insulating phase ($\nu := t/U < 1$) and a phase with extended phonon wavefunctions ($\nu > 1$), the critical point being at $\nu_c = 1$ for a nearest-neighbor model.

Additionally, the disorder-averaged local density of states (LDOS) has a different behavior in the two regimes [26]. Thus, such a phase transition can be detected in the phonon LDOS $\rho_j(\omega) = \langle \sum_n \mathcal{M}_{jn}^2 \delta(\omega - \omega_L - \Omega_n) \rangle$ by means of the fluorescence spectrum when the laser is focused on a single ion $\mathcal{S}_-(\omega) \propto \rho_j(\omega)$. We emphasize that ion traps not only allow an ideal realization of the RDM, but also suggest the possibility of engineering a wide range of disorder correlations that surpass real materials.

### *4.2. Bose-glass phase*

Finally, radial anharmonicities in the trapping potentials can be enhanced by an additional standing wave [9]. These nonlinearities lead to repulsive (attractive) on-site interactions between the phonons whenever the ions sit at the maxima (minima) of the standing-wave laser. Combining these interactions with the effective Hamiltonian in equation (5), one reaches the disordered strongly correlated model

$$H_{\text{eff}}^{\{s\}} = \sum_{jk} t_{jk} a_j^\dagger a_k + \sum_j \varepsilon_j(\{\boldsymbol{s}\}) a_j^\dagger a_j + \sum_j U (a_j^\dagger)^2 a_j^2, \tag{8}$$

where the interaction strength $U$ can be controlled by the laser parameters [9]. Accordingly, it is possible to study the fate of Anderson localization in the presence of disorder, where a yet to be observed insulating phase arises: the Bose glass [6, 27]. In contrast to the Mott insulator that arises due to the suppression of density fluctuations in the strong repulsive regime, the Bose glass is a gapless and compressible phase, but still an insulator due to disorder localization. Trapped ions are to be considered as an attractive platform to realize and detect these different phases. In fact, they are well suited to distingish experimentally between Mott-insulating and Bose-glass phases. Following [28], it is possible to infer the compressibility via measurements of the boson distribution under modifications of a confining potential. For trapped ions, the phonons are harmonically confined to the center of the Coulomb crystal, which can be modified by tuning the trapping frequency or the ion number [9]. Under these variations, the phonon distribution can be measured using standard techniques [7] and thus the compressibility inferred.

## 5. Conclusions

We have presented a scheme that uses ion crystals to measure phonon localization induced by disorder. We have shown that measuring the collective resonance fluorescence suffices to prove Anderson localization, which can be surprisingly observed even at high phonon temperatures.

## Acknowledgments

We acknowledge support from EU grant PICC (Physics with Ion Coulomb Crystals), QUITEMAD S2009-ESP-1594, FIS2009-10061, CAM-UCM/910758, FPU MEC grant and RyC Y200200074. DP thanks A V Malyshev, K Singer and J Eschner for useful discussions.

## References


[1] Anderson P W 1958 *Phys. Rev.* **109** 1492
[2] Kramer B and MacKinnon A 1993 *Rep. Prog. Phys.* **56** 1469
[3] Wiersma D S *et al* 1997 *Nature* **390** 671
Schwartz T *et al* 2007 *Nature* **446** 52
[4] Hu H *et al* 2008 *Nat. Phys.* **4** 945
[5] Billy J *et al* 2008 *Nature* **453** 891
Roati G *et al* 2008 *Nature* **453** 895
[6] Sanchez-Palencia L and Lewenstein M 2010 *Nat. Phys.* **6** 87
[7] Leibfried D *et al* 2003 *Rev. Mod. Phys.* **75** 281
[8] Porras D and Cirac J I 2004 *Phys. Rev. Lett.* **92** 207901
[9] Porras D and Cirac J I 2004 *Phys. Rev. Lett.* **93** 263602
[10] Retzker A *et al* 2008 *Phys. Rev. Lett.* **101** 260504
[11] Ivanov P A *et al* 2009 *Phys. Rev.* A **80** 060301
[12] Friedenauer A *et al* 2008 *Nat. Phys.* **4** 757
[13] Kim K *et al* 2009 *Phys. Rev. Lett.* **103** 120502
[14] Schmidt-Kaler F *et al* 2004 *Europhys. Lett.* **65** 587
[15] Ivanov P A, Vitanov N V, Singer K and Schmidt-Kaler F 2010 arXiv:1002.3033
[16] Paredes B, Verstraete F and Cirac J I 2005 *Phys. Rev. Lett.* **95** 140501
Roscilde T and Cirac J I 2007 *Phys. Rev. Lett.* **98** 190402
[17] Törma P, Jex I and Schleich W P 2002 *Phys. Rev.* A **65** 052110
[18] Velický B, Kirkpatrick S and Ehrenreich H 1968 *Phys. Rev.* **175** 747
[19] Cirac J I and Zoller P 1995 *Phys. Rev. Lett.* **74** 4091
Leifried D *et al* 2003 *Nature* **422** 412
Schmidt-Kaler F *et al* 2003 *Nature* **422** 408
[20] Mott N F and Twose W D 1961 *Adv. Phys.* **10** 107
[21] Meekhof D M *et al* 1996 *Phys. Rev. Lett.* **76** 1796
[22] Raab Ch *et al* 2000 *Phys. Rev. Lett.* **85** 538
[23] Cirac J I *et al* 1992 *Phys. Rev.* A **46** 2668
Cirac J I *et al* 1993 *Phys. Rev.* A **48** 2169
[24] Scully M O and Zubairy M S 1997 *Quantum Optics* (Cambridge: Cambridge University Press)
[25] Dunlap D H *et al* 1990 *Phys. Rev. Lett.* **65** 88
Bellani V *et al* 1999 *Phys. Rev. Lett.* **82** 2159
[26] Evangelou S N and Wang A Z 1993 *Phys. Rev.* B **47** 13126
[27] Fisher M P A *et al* 1989 *Phys. Rev.* B **40** 546
[28] Delande D and Zakrzewski J 2009 *Phys. Rev. Lett.* **102** 085301
Roscilde T 2009 *New J. Phys.* **11** 023019